Supplementary Information

Concentration dependent halogen-bond density in the 2D self-assembly of thienophenanthrene derivative at the aliphatic acid/graphite interface

Bao Zha, Xinrui Miao*, Pei Liu, Yumeng Wu and Wenli Deng*

College of Materials Science and Engineering, South China University of Technology, Guangzhou 510640, China

Experimental Section

1. General Information

^{1}H and ^{13}C NMR spectra were recorded out on a Bruker AV-400 MHz/Avance Ⅱ 600MHz NMR spectrometer. Mass spectra were determined using a Esquire HCT PLUS instrument. Infrared spectra were obtained with a LabRAM Aramis spectrometer.

2. Synthesis and Characterization of (4) DDTD and (5) DPTD

2.1. Scheme1. Compound 4

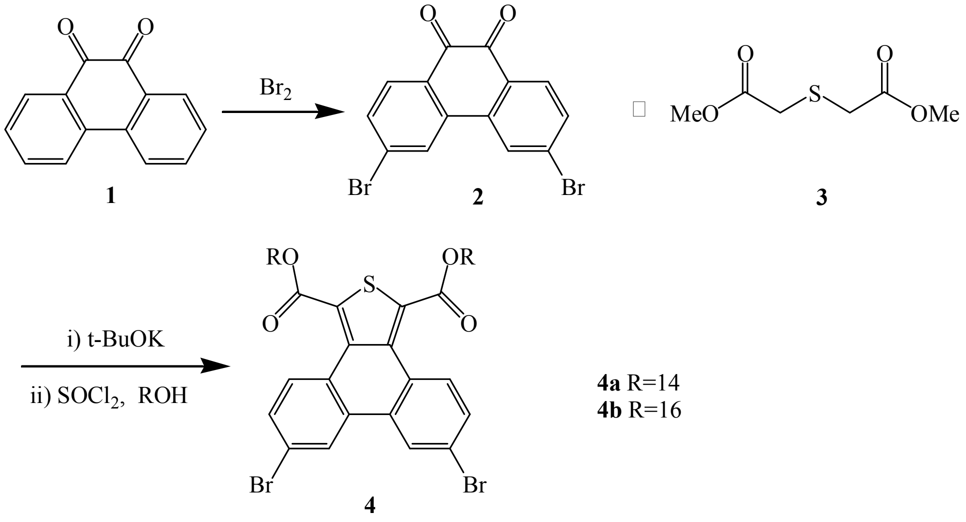

3,6-Dibromo-9,10-phenanthrenequinone **2,** and acetic acid, 2,2'-thiobis-1, 1'-dimethyl ester **3** were synthesized as previously reported in the literatures.[1-2]

Compound 4a Phenanthrenequinone (2.08 g, 10.00 mmol), Br_2 (2.50 mL, 49.25 mmol), and benzoyl peroxide (1 g) were added to nitrobenzene (20.0 mL). The mixture was exposed to a 250 W tungsten lamp for 3 h. After 30 min, the mixture was cooled to room temperature and filtered. The crude product was washed with MeOH and H_2O, and dried under vacuum to give **2**. A mixture of **2** (1.09 g, 2.98 mmol) and **3** (0.54 g, 3.1 mmol) were transferred to a dry 250 mL round-bottom flask and then dissolved in benzene (60 mL) under an atmosphere of nitrogen. After gradually adding a solution of t-BuOK (1.68 g, 15 mmol) in methanol (10 ml), the green dark brown suspension was stirred at room temperature for 5 days. The reaction mixture was poured into H_2O (100 mL) and the organic solvent was removed under reduced pressure. Washing the product with HCl gave a yellow solid. Thereafter, the yellow solid was dissolved in $SOCl_2$ (8 mL) and the reddish-colored reaction mixture was stirred at 80 ºC for 6 h. The $SOCl_2$ was removed under reduced pressure. n-Tetradecanol (2.57 g, 12 mmol) and THF (10 mL) were added to the mixture, which was stirred at 100 ºC for 2 h. The solvent was removed by vacuum. The crude product was subjected to column chromatography (20％ EA/PE) to give **4a** as a cyan solid.

Data for 4a. ^{1}H NMR (600 MHz, $CDCl_3$, ppm): δ 8.85 (2H, m), 8.49 (2H, m), 7.66 (2H, m), 4.46 (4H, m), 1.84 (4H, m), 1.50 (4H, m), 1.23 (40H, m), 0.90 (6H, m). ^{13}C NMR (150 MHz, $CDCl_3$): δ 163.02, 137.24, 131.62, 130.66, 129.95, 128.97, 126.19, 125.77, 123.31, 66.62, 31.92, 29.70, 29.69, 29.66, 29.59, 29.54, 29.36, 29.25, 28.58, 26.02, 22.69, 14.12. FT-IR (KBr, cm^{-1}): v 2931, 2925, 2844, 1712, 1596, 1539, 1508, 1466, 1408, 1390, 1302, 1265, 1250, 1223, 1174, 1147, 1135, 1074, 1029, 995, 962, 925, 889, 859, 810, 769, 719, 655, 613, 573, 513, 461. MS (APCI): calcd. for $C_{46}H_{64}Br_2O_4S$: 872. Found: 872 (m/z + H^+).

Compound 4b Phenanthrenequinone (2.08 g, 10.00 mmol), Br_2 (2.50 mL, 49.25 mmol), and benzoyl peroxide (1 g) were added to nitrobenzene (20.0 mL). The mixture was exposed to a 250 W tungsten lamp for 3 h. After 30 min, the mixture was cooled to room temperature and filtered. The crude product was washed with MeOH and H_2O, and dried under vacuum to give **2**. A mixture of **2** (1.09 g, 2.98 mmol) and **3** (0.54 g, 3.1 mmol) were transferred to a dry 250 mL round-bottom flask and then dissolved in benzene (60 mL) under an atmosphere of nitrogen. After gradually adding a solution of t-BuOK (1.68 g, 15 mmol) in methanol (10 ml), the green dark brown suspension was stirred at room temperature for 5 days. The reaction mixture was poured into H_2O (100 mL) and the organic solvent was removed under reduced pressure. Washing the product with HCl gave a yellow solid. Thereafter, the yellow solid was dissolved in $SOCl_2$ (8 mL) and the reddish-colored reaction mixture was stirred at 80 ºC for 6 h. The $SOCl_2$ was removed under reduced pressure. n-Hexadecanol (2.91 g, 12 mmol) and THF (10 mL) were added to the mixture, which was stirred at 100 ºC for 2 h. The solvent was removed by vacuum. The crude product was subjected to column chromatography (20％ EA/PE) to give **4b** as a cyan solid.

Data for 4b. ^{1}H NMR (400 MHz, $CDCl_3$, ppm): δ 8.79 (2H, m), 8.45 (2H, m), 7.62 (2H, m), 4.43 (4H, m), 1.83 (4H, m), 1.47 (4H, m), 1.25 (48H, m), 0.88 (6H, m). ^{13}C NMR (100 MHz, $CDCl_3$): δ 164.29, 138.51, 132.84, 131.93, 131.22, 130.23, 130.16, 127.46, 126.98, 124.59, 67.91, 33.22, 31.00, 30.89, 30.85, 30.66, 30.55, 29.87, 27.32, 23.99, 15.42. FT-IR (KBr, cm^{-1}): v 2952, 2917, 2849, 1712, 1642, 1540, 1510, 1469, 1406, 1391, 1301, 1247, 1177, 1143, 1094, 1027, 944, 886, 865, 812, 763, 719, 617. MS (APCI): calcd. for $C_{50}H_{72}Br_2O_4S$: 928. Found: 927 (m/z + H^+).

2.2. Scheme2. Synthesis of Compound 5

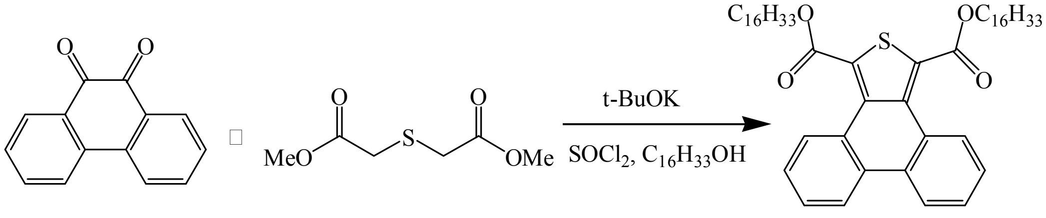

1 3 5

Compound 5 A mixture of **1** (0.61 g, 2.98 mmol) and **3** (0.54 g, 3.1 mmol) were transferred to a dry 250 mL round-bottom flask and then dissolved in benzene (60 mL) under an atmosphere of nitrogen. After gradually adding a solution of t-BuOK (1.68 g, 15 mmol) in methanol (10 ml), the dark brown suspension was stirred at room temperature for 5 days. The reaction mixture was poured into H_2O (100 mL) and the organic solvent was removed under reduced pressure. Washing the product with HCl gave a yellow solid. Thereafter, the yellow solid was dissolved in $SOCl_2$ (8 mL) and the reddish-colored reaction mixture was stirred at 80 ºC for 6 h. The $SOCl_2$ was removed under reduced pressure. n-Hexadecanol (2.91g, 12mmol) and THF (10 mL) were added to the mixture, which was stirred at 100 ºC for 2 h. The solvent was removed by vacuum. The crude product was subjected to column chromatography (25％ EA/PE) to give **5** as a turquoise solid.

Data for 5. ^{1}H NMR (400 MHz, $CDCl_3$, ppm): δ 8.86 (2H, m), 8.44 (2H, m), 7.62 (2H, m), 7.53 (2H, m), 4.44 (4H, m), 1.83 (4H, m), 1.48 (4H, m), 1.25 (48H, m), 0.88 (6H, m). ^{13}C NMR (100 MHz, $CDCl_3$): δ 164.80, 139.53, 132.40, 129.99, 129.61, 129.46, 128.35, 128.03, 124.61, 67.71, 33.23, 31.00, 30.89, 30.84, 30.66, 30.56, 29.89, 27.33, 23.99, 15.42. FT-IR (KBr, cm^{-1}): v 2953, 2914, 2849, 1713, 1641, 1513, 1471, 1411, 1381, 1320, 1254, 1222, 1160, 1127, 1094, 1064, 945, 867, 745, 716, 610. MS (APCI): calcd. for $C_{50}H_{74}O_4S$: 770. Found: 770 (m/z + H^+).

3. Scanning tunneling microscopy (STM)

1-Heptoic acid (TCI), 1-octanoic acid (TCI) and **1-**nonoic acid (TCI) were used as received. The molecule (0.1 mg) dissolved in 1 mL of solvents was used for preparing the solution. The solution with sediment was sonicated in an ultrasonic bath for 1 h. The concentration of solution increases and eventually reaches saturated. The supernatant saturated solution was used as the mother solution. Different solution concentrations were obtained by continuously diluting the mother solution.

The samples were prepared by dropping a droplet (~ 1 μL) of solution that contained DDTD or DPTD (concentration: 10^{-3}~ 10^{-6} mol L^{-1}) onto a freshly cleaved atomically flat surface of HOPG (quality ZYB, Bruker, USA). Most images obtained at the liquid/solid interface were recorded within 3 h after dropping a solution.

STM measurements were performed on a Nanoscope Ⅲa Multimode SPM (Bruker, USA) at ambient conditions (15 and 30 ºC, respectively) with the tip immersed in the supernatant liquid. The tips were mechanically cut from Pt/Ir wires (80/20). All the images were recorded with the constant current mode and are shown without further processing. The tunneling parameters are given in the corresponding figure caption. Different tips and samples were used to check the reproducibility and to exclude image artifact that were caused by the tips or the samples. The HOPG lattice was used as an internal standard to correct each STM images and to determine the average lattice parameters of the DDTD or DPTD monolayer by examining at least 4 images.

4. Computational simulation

Molecular models of the assembled structures were built by Materials Studio 4.4. The model of monolayer was constructed by placing the molecules according to the intermolecular distances and angles that were obtained from the analysis of STM images. Semiempirically calculated spatial distribution of the HOMO for DDTD and DPTD is performed by Gaussion 03W.

DFT calculations were performed with Gaussian 03 software package. All the geometry full-optimization of those structures were done through the hybrid B3LYP method together with the split-valence polarized 6-31G(d) basis set. The B3LYP functional has been found to provide good agreement with experimental results for the adsorption of organic molecules on different surface.[3,4] The 6-31G(d) basis set was found to provide the lowest total energy and to be more suitable for modeling hydrogen bonded (ad) species.[5] Halogen bond is similar to hydrogen bond known as a kind of non-covalent intermolecular interaction.

References:

[1] Bhatt, M. V. Tetrahedron 1964, 20, 803.

[2] Kim, M.; Yoo, J.; Im, H.; Kim, Synthetic Metals 2012, 162, 2361-2369.

[3] Tao, F.; Qiao, M.; Li, Z.; Yang, L.; Dai, Y.; Huang, H.; Xu, G. Phys. Rev. B. 2003, 67,1−7.

[4] Wolkow, R. A. Rev. Phys. Chem. 1999, 50, 413−441.

[5] Chatterjee, A.; Zhang, L.; Leung, K. T. Langmuir. 2013, 29 , 9369-9377.

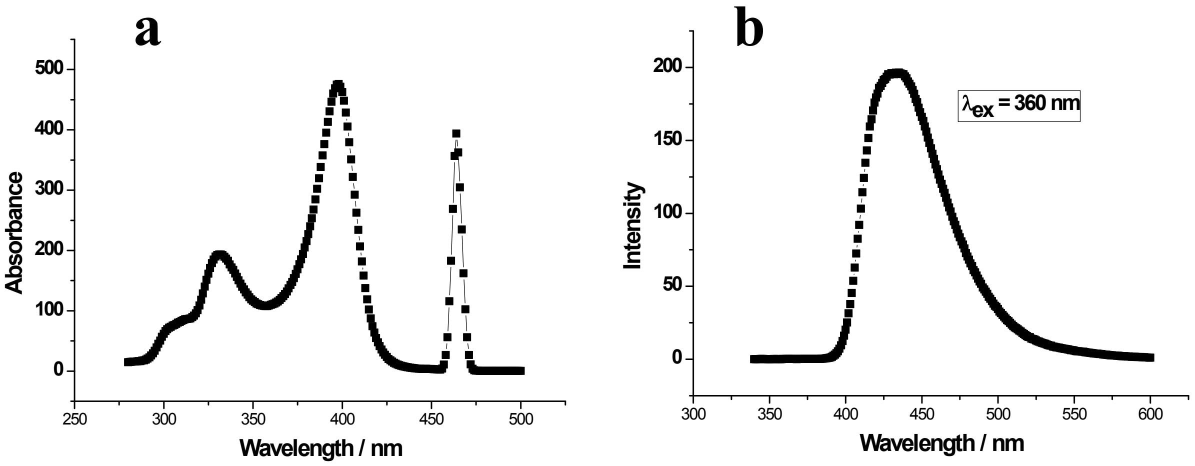

Fig. S1 Solution adsorption spectrum of DDTD in dichloromethane (a) and emission spectrum of DDTD (b).

(1) Self-assembly of DDTD in 1-octanoic acid

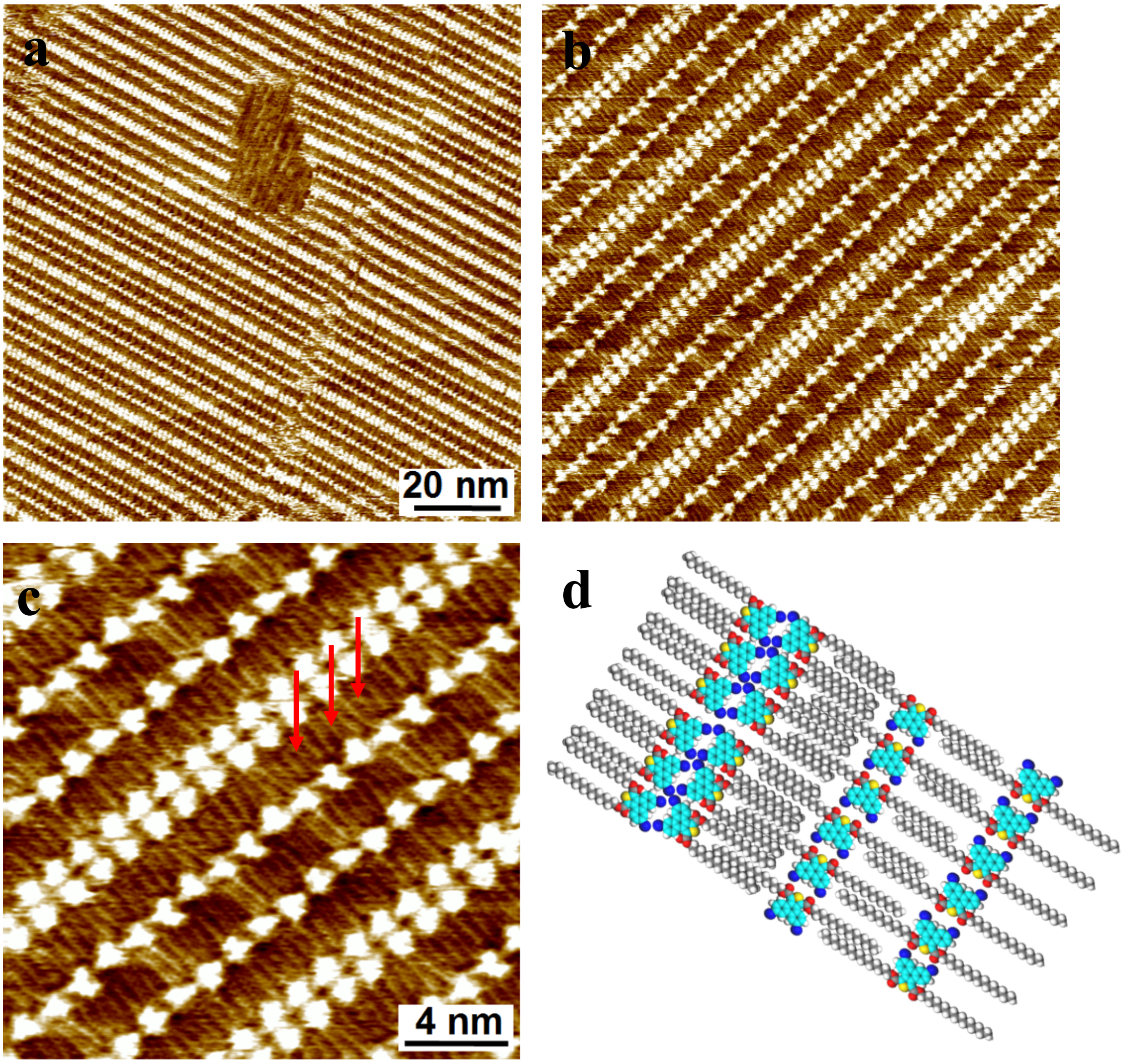

Fig. S2 Large–scale (a) and small-scale (b) (50 × 50 nm^2) STM images of DDTD under a high concentration (saturated solution) at the 1-octanoic acid/graphite interface. V_{bias} = 560 mV, I_t = 430 pA. (c) High-resolution STM image of DDTD under a high concentration (saturated solution) at the octanoic acid/graphite interface. V_{bias} = 580 mV, I_t = 400 pA. (d) Molecular model illustrating the self-assembly pattern based on the STM image. The ambient temperature is 15 ºC.

From the molecular model, we can observe that two alkyl chains are present in the alkyl lamella between single core columns. However, the alkyl chain density appears to be similar in both types of alkyl lamellae. Only between the single core columns, apparent Moiré effect was observed. The dark area probably is the graphite lattice.

The length of side chain of DDTD is about 2.0 nm.

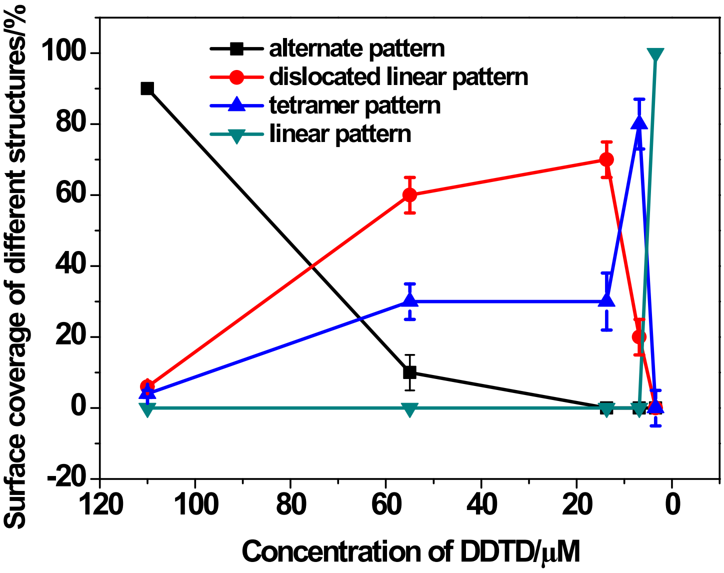

Fig. S3 Concentration dependence of the surface coverage of different patterns at the 1-octanoic acid/graphite interface. The labels refer to the different patterns of DDTD in the drop-casting solution.

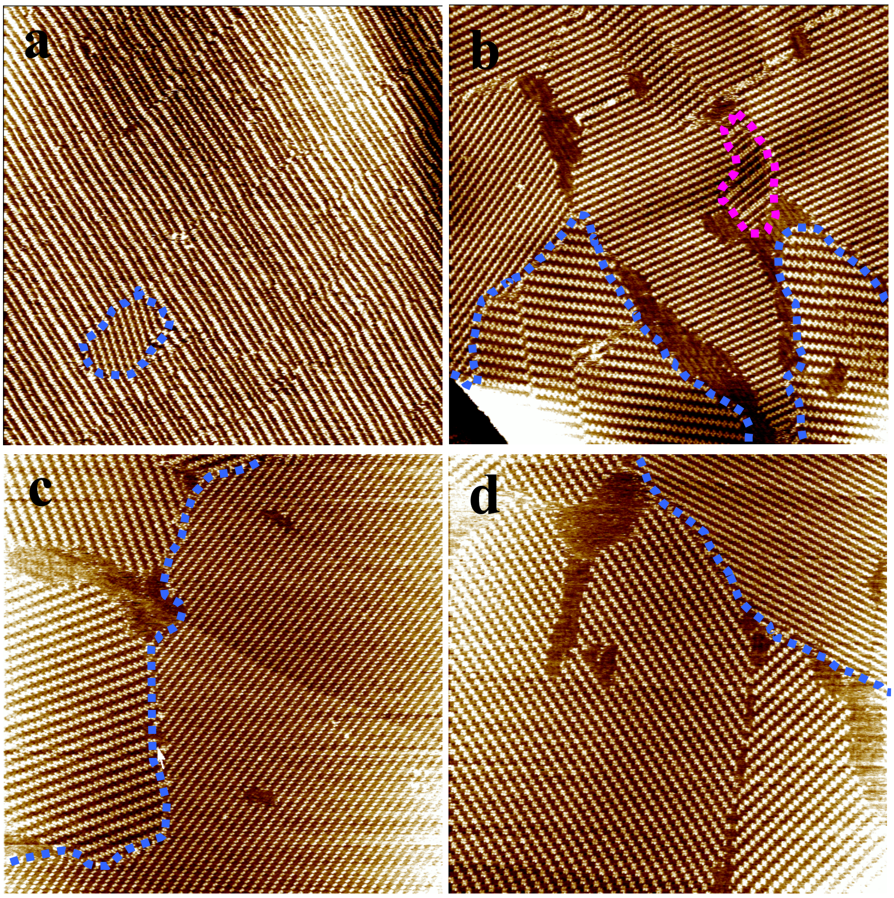

Fig. S4 Large-scale (200 × 200 nm^2) STM images of DDTD self-assembled patterns under different concentrations 1-octanoic acid/graphite interface. (a) 1.1 × 10^{-3} mol L^{-1}; (b) 5.5 × 10^{-4} mol L^{-1}; (c) 1.37 × 10^{-4} mol L^{-1}; (d) 6.85 × 10^{-5} mol L^{-1}. Ambient temperature is 15 ºC. V_{bias} = 500-600 mV, I_{t} = 400-450 pA.

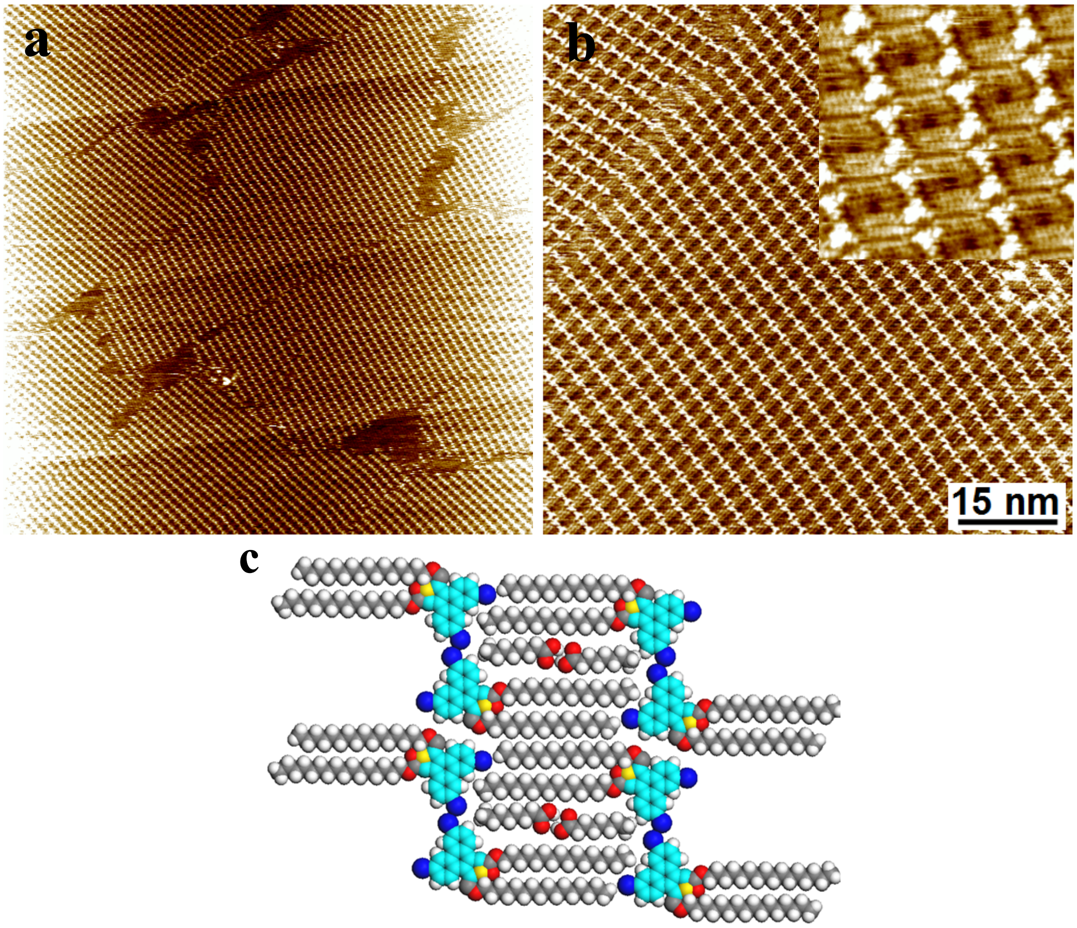

Fig. S5 (a) Large-scale (200 × 200 nm^2) and (b) small-scale STM images of DDTD monolayer under low concentrations at the1-octanoic acid/graphite interface. Concentration: 3.4 × 10^{-5} mol L^{-1} V_{bias} = 575 mV, I_{t} = 423 pA. (c) Molecular model illustrating the self-assembly pattern based on the STM image. The ambient temperature is 15 ºC.

A carefully observation from Fig. S6b demonstrates that there is a kind of dark chain with a darker hole between the side chains, which corresponds to two 1-octanoic acid molecules with a length of 1.92 nm.

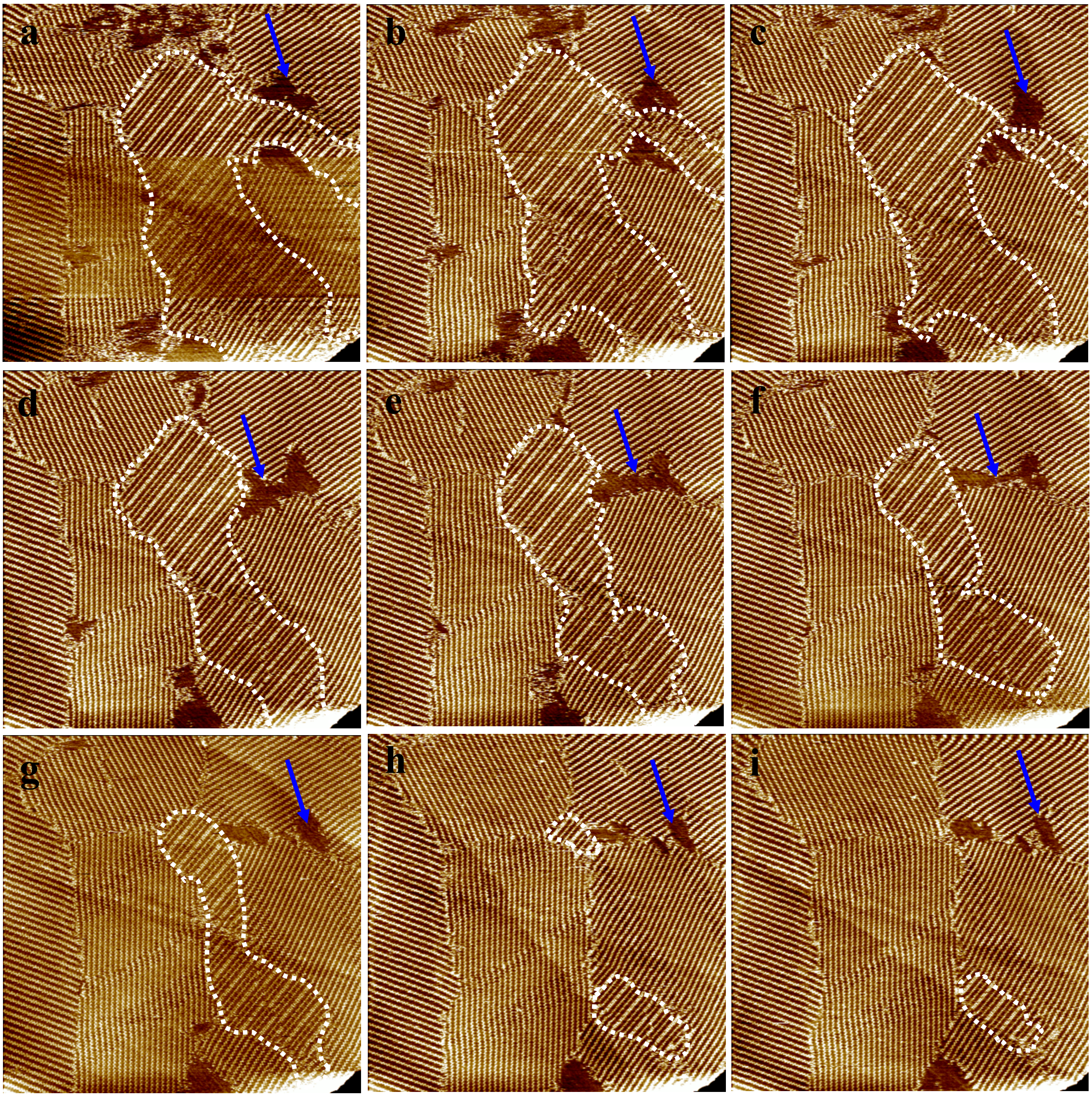

Fig. S6 A sequence of STM images recorded in the same area depicting a gradual transformation of the alternate structure to the dislocated linear structure at the 1-octanoic acid/graphite interface. (Scan area 200 × 200 nm^2.) The dashed bright line depicts the phase boundary. It can be noticed that contour of the phase boundary changes gradually with time which indicates that this is not an effect observed due to scanner drift. Moreover, the fuzzy region around this boundary and the shrink of dark voids demonstrate the dynamic nature of molecules adsorbed in that region. Imaging conditions: $V_{\mathrm{bias}} = 540$ mV, $I_{\mathrm{t}} = 390$ pA. The ambient temperature is 15 ºC.

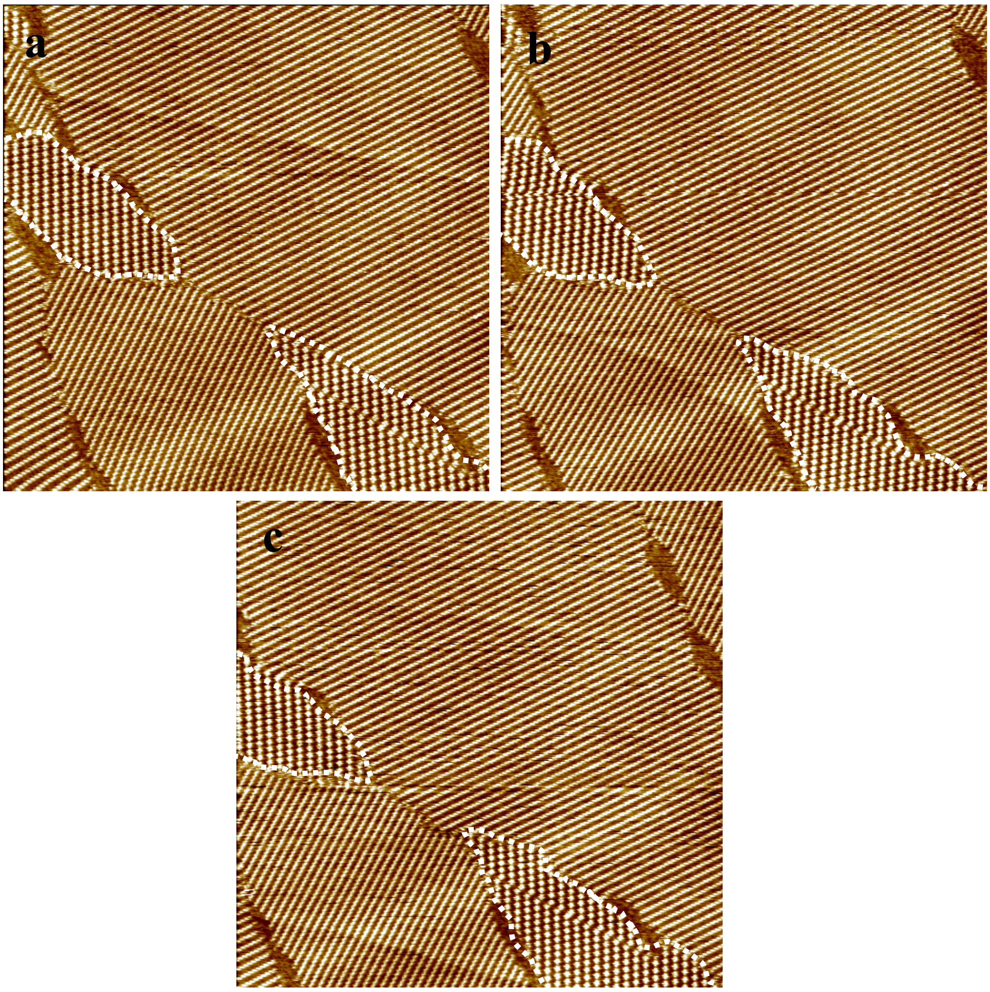

Fig. S7 A sequence of STM images recorded in the same area depicting no structural transformation between the dislocated linear structure and tetramer structure. (Scan area 200 × 200 nm^2.) The dashed bright line depicts the phase boundary.

(2) Self-assembly of DDTD in 1-heptoic acid

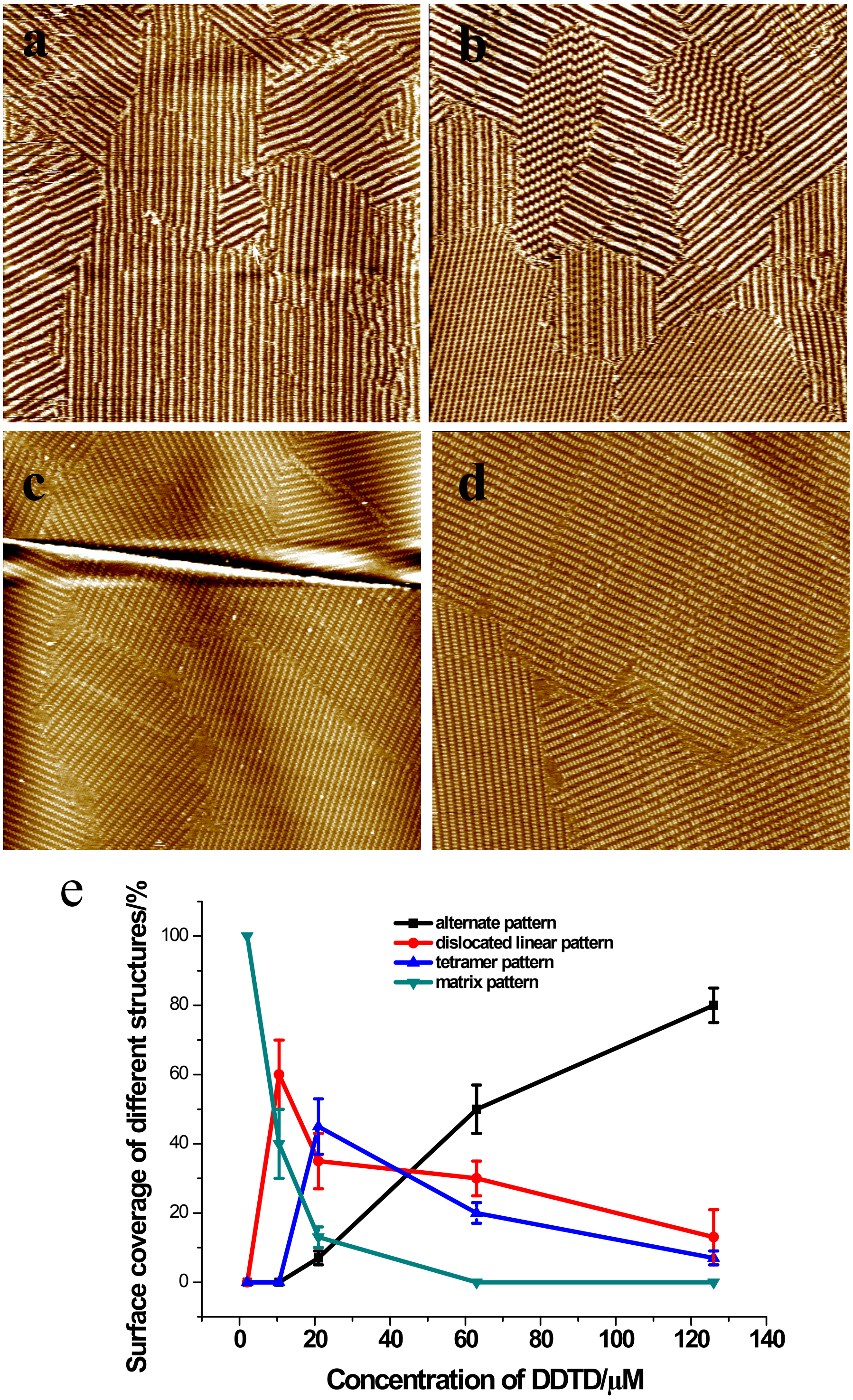

Fig. S8 Representative large-scale (200 × 200 nm^2) STM images of DDTD self-assembled patterns under different concentrations at the 1-heptoic acid/graphite interface. (a) 1.26 × 10^{-3} mol L^{-1}; (b) 6.3 × 10^{-4} mol L^{-1}; (c) 1.05 × 10^{-4} mol L^{-1}; (d) 2.1 × 10^{-5} mol L^{-1}. Ambient temperature is 20 ºC. V_{bias} = 500-600 mV, I_{t} = 400-450 pA. The images were recorded immediately after the solution was dropped on the graphite surface. (f) Concentration dependence of the surface coverage of different patterns. The labels refer to the different patterns of DDTD in the drop-casting solution.

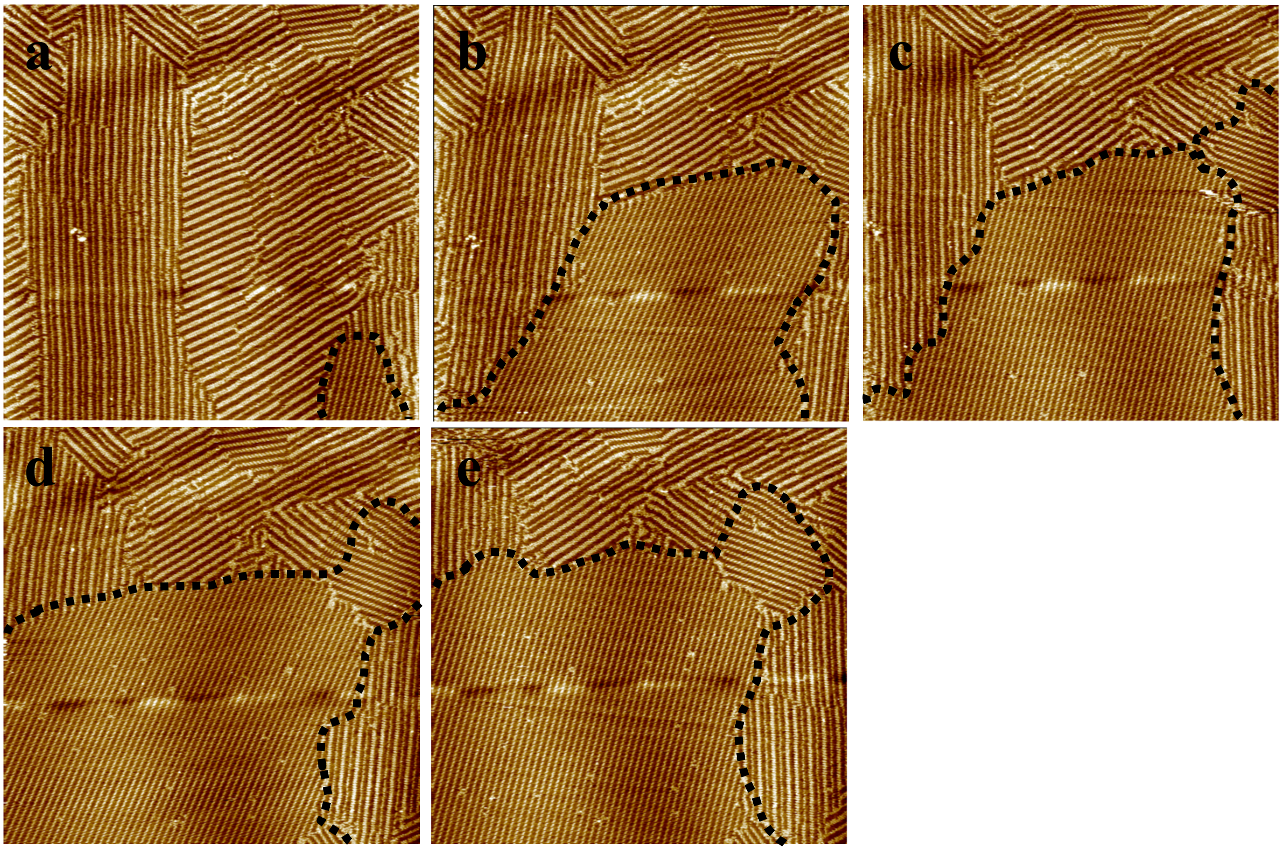

Fig. S9 A sequence of STM images recorded in the same area depicting a gradual transformation of the alternate structure to the dislocated linear structure at the 1-heptoic acid/graphite interface (1.26 × 10^{-3} mol L^{-1}). (Scan area 200 × 200 nm^2.) The dashed bright line depicts the phase boundary. It can be noticed that contour of the phase boundary changes gradually with time which indicates that this is not an effect observed due to scanner drift. Moreover, the fuzzy region around this boundary and the shrink of dark voids demonstrate the dynamic nature of molecules adsorbed in that region. Imaging conditions: V_{bias} = 610 mV, I_{t} = 430 pA. The ambient temperature is 20 ºC.

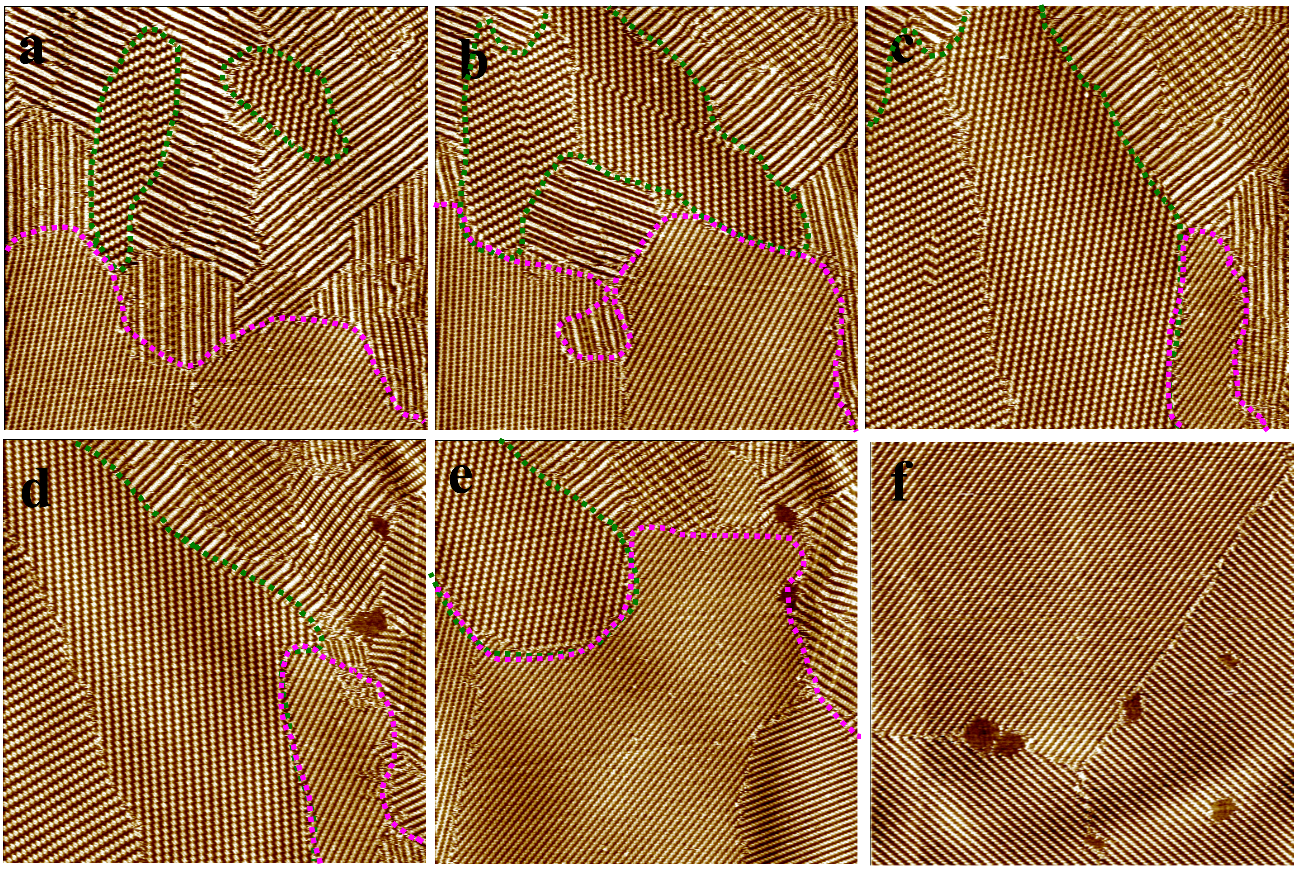

Fig. S10 (a-e) A sequence of STM images recorded in the same area depicting a gradual transformation of the alternate structure to the dislocated linear and tetramer structures at the 1-heptoic acid/graphite interface (6.3 × 10^{-4} mol L^{-1}). Scan area: 200 × 200 nm^2. Moreover, the structural transformation from the tetramer pattern to the dislocated linear pattern was recorded. The dashed bright line depicts the phase boundary. It can be noticed that contour of the phase boundary changes gradually with time which indicates that this is not an effect observed due to scanner drift. Imaging conditions: $V_{\text{bias}} = 610$ mV, $I_t = 430$ pA. The ambient temperature is 20 ºC. (f) The STM image after repeated scanning in the same area.

Under a relative high concentration (6.3 × 10^{-4}

mol L^{-1}), the structural transition form the alternate pattern to the tetramer pattern was observed. However, with the continuous scanning, the tetramer pattern was transformed into the dislocated linear pattern. The result indicates that the dislocated linear pattern is the most stable under the concentration.

(3) Self-assembly of DDTD in 1-nonoic acid

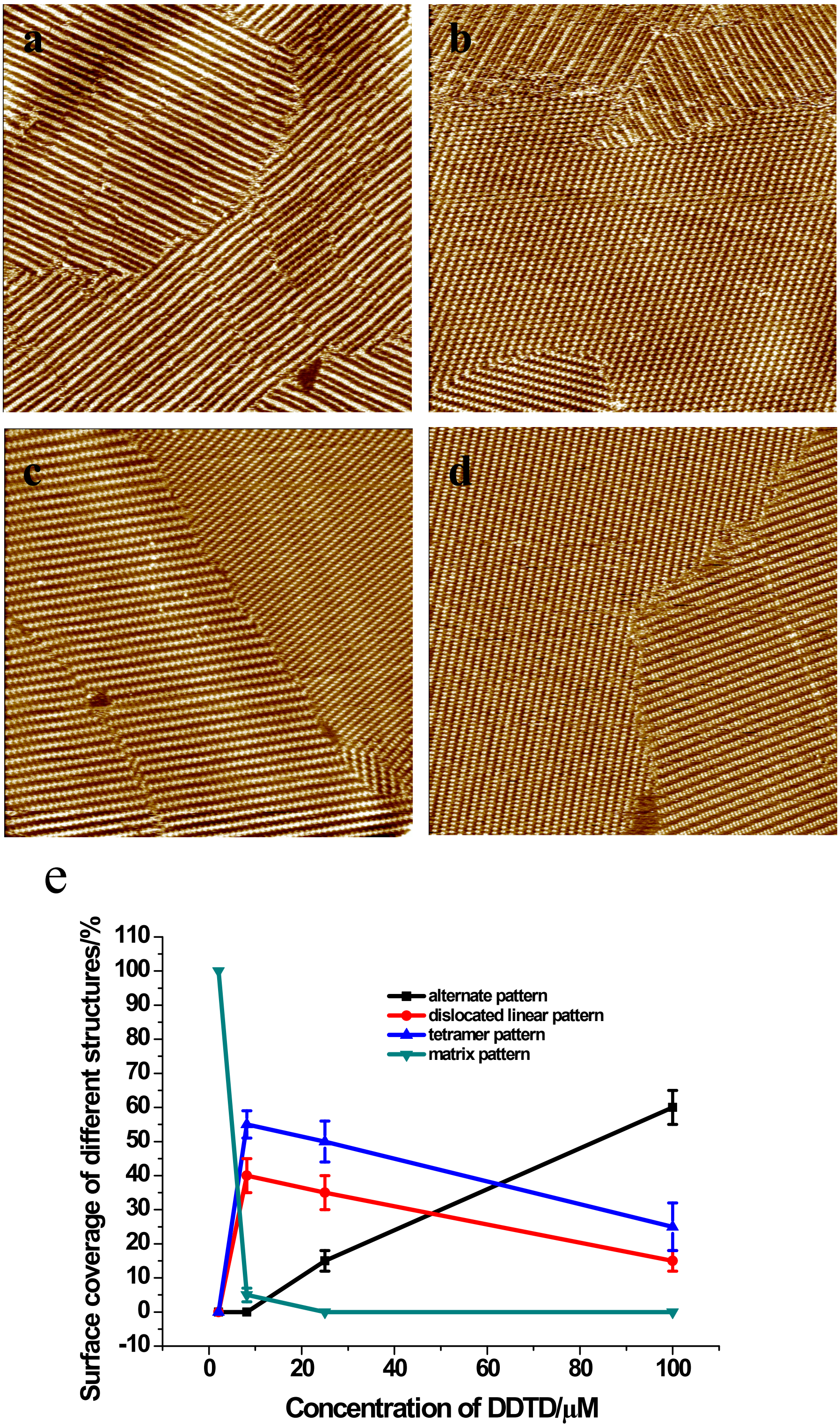

Fig. S11 Representative large-scale (200 × 200 nm^2) STM images of DDTD self-assembled patterns under different concentrations at the 1-nonoic acid/graphite interface. (a) 1.0 × 10^{-3} mol L^{-1}; (b) 2.5 × 10^{-4} mol L^{-1}; (c) 8.2 × 10^{-5} mol L^{-1}; (d) 2.1 × 10^{-5} mol L^{-1}. Ambient temperature is 20 ºC. V_{bias} = 500-600 mV, I_t = 400-450 pA. (f) Concentration dependence of the surface coverage of different patterns. The labels refer to the different patterns of DDTD in the drop-casting solution.

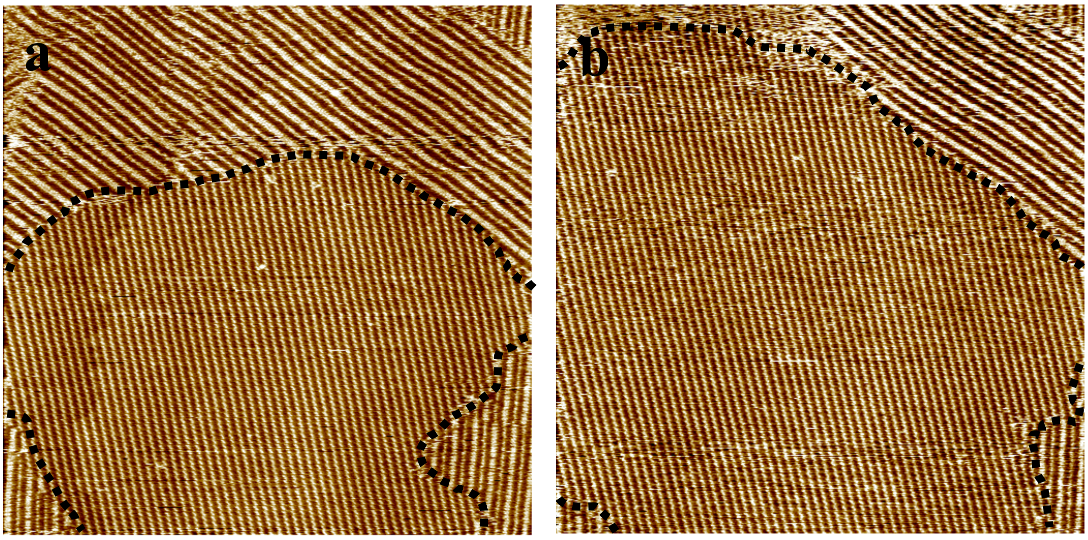

Fig. S12 A sequence of STM images recorded in the same area depicting a gradual transformation of the alternate structure to the dislocated linear structure at the 1-nonoic acid/graphite interface (6.3 × 10^{-4} mol L^{-1}). (Scan area 200 × 200 nm^2.) The dashed bright line depicts the phase boundary.

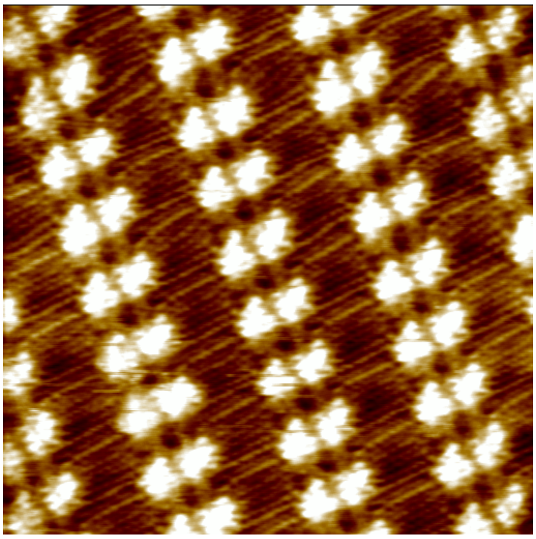

Fig. S13 STM image (15 × 15 nm^2) of the DDTD adlayer in 1-nonoic acid under a low concentration (2.5 × 10^{-5} M). V_{bias} = 600 mV, I_t = 400 pA.

The solubility of DDTD molecule in acid is low, so the saturated concentration is about 10^{-3} mol L^{-1}. The polarity of the solvent is 1-heptoic acid>1-octanoic acid>1-nonoic acid. The solubility of DDTD molecule in 1-heptoic acid is the highest. Thus, the coexistence of four kinds of patterns was observed.

(4) Self-assembly of DPTD in 1-octanoic acid

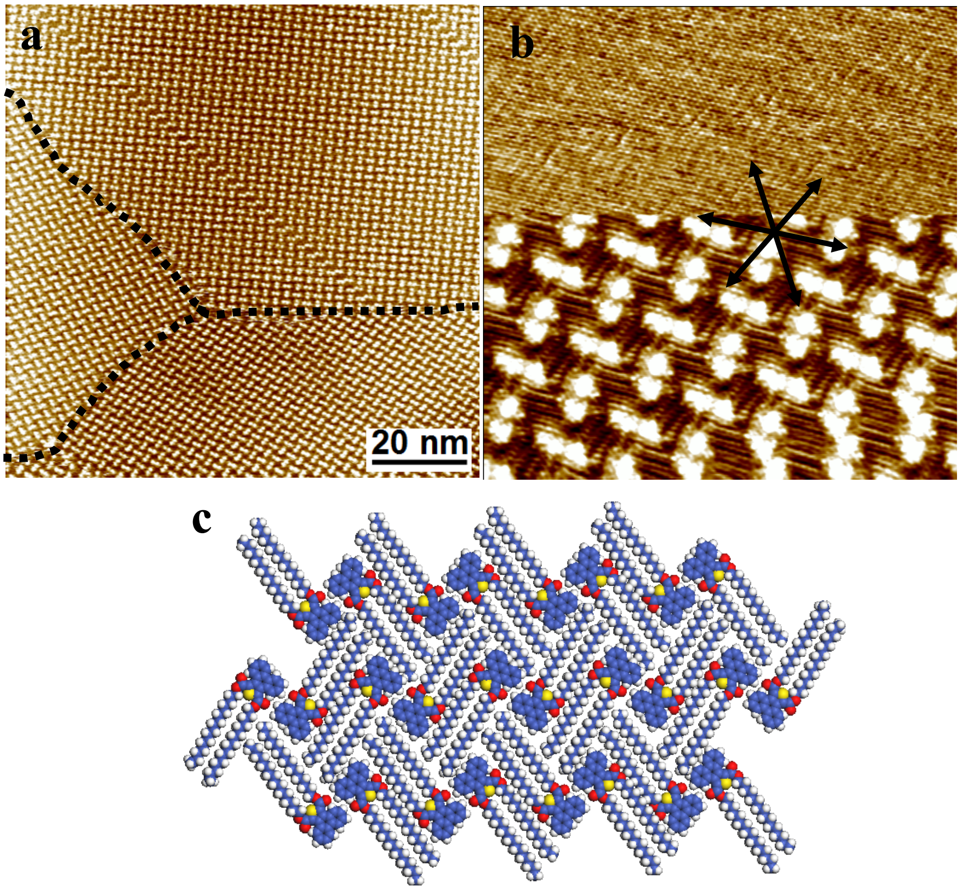

Fig. S14 (a) Large-scale STM image of the DPTD monolayer at the 1-octanoic acid/graphite interface. V_{bias} = 580 mV, I_t = 410 pA. (b) Composite STM image (18 × 18 nm^2) showing the underlying HOPG lattice and the windmill-shaped structure. V_{bias} = 560 mV, I_t = 400 pA for the molecular adlayer (Lower) and V_{bias} = 100 mV, I_t = 400 pA for the HOPG lattice (Upper). The image was obtained by switching the bias during the STM scan from the bottom to the upper frame. (c) Molecular model illustrating the self-assembly pattern based on the STM image.

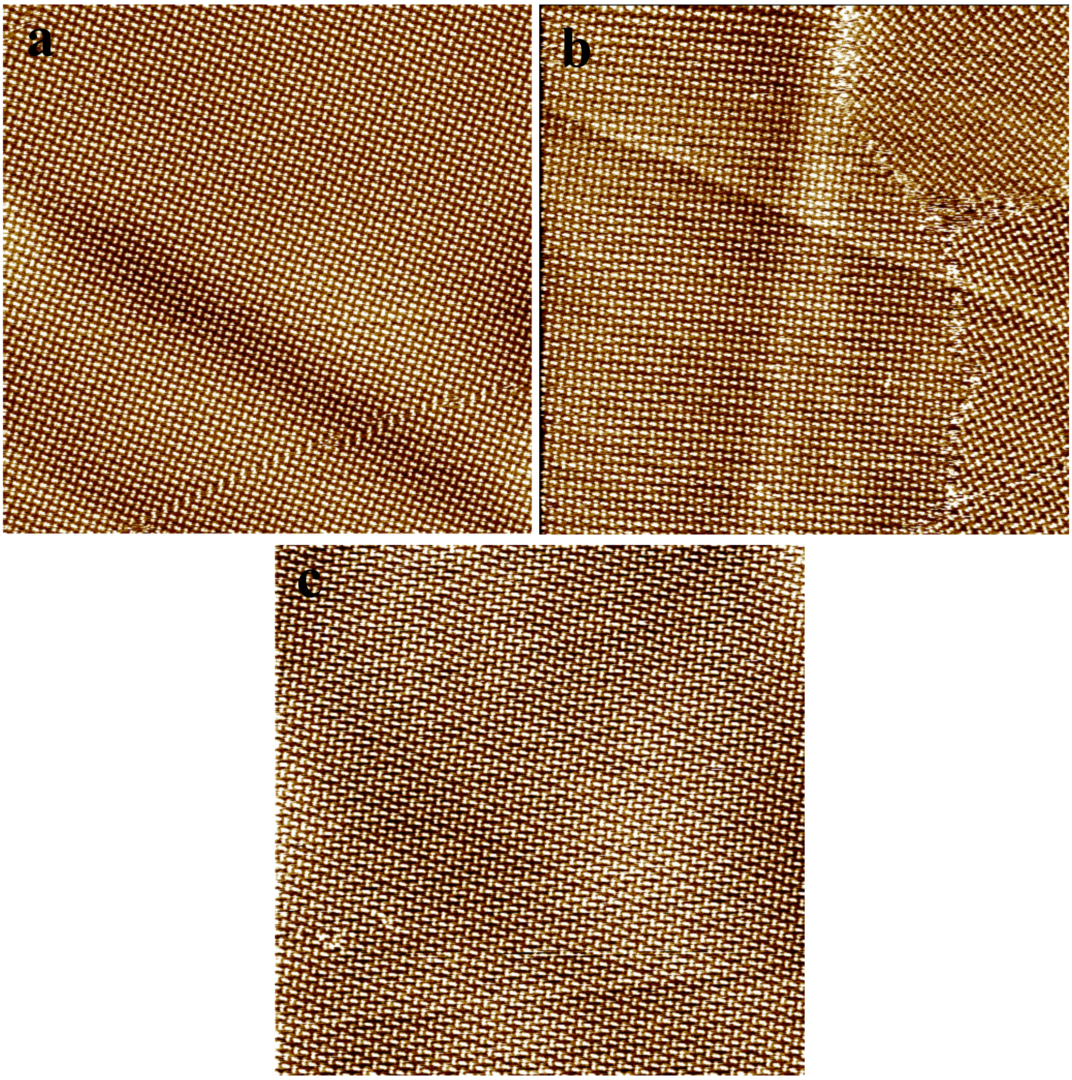

Fig. S15 Large-scale (150 × 150 nm^2) STM images of DPTD self-assembled patterns under different concentrations. (a) 3.0 × 10^{-3} mol L^{-1}; (b) 5.0 × 10^{-4} mol L^{-1}; (c) 6.2 × 10^{-5} mol L^{-1}. Ambient temperature is 15 ºC. V_{bias} = 500-600 mV, I_{t} = 400-450 pA.

Table S1. Summary of Structural Parameters of the 2D Nanopatterns Assembled by DDTD and DPTD.

molecule	Structure	a (nm)[A]	b (nm)[B]	γ (°)[C]	Molecular density(nm^2/molecule)	Bonding energy (kcal/mol)
DDTD	Alternate pattern	-	-	-	3.13	
	Dimer pattern	2.3 ± 0.1	3.7 ± 0.1	78 ± 1	3.75	−7.41
	Tetramer pattern	2.8 ± 0.1	6.7 ± 0.1	45 ± 1	3.75	−22.04
	Linear pattern	2.6 ± 0.1	3.6 ± 0.1	77 ± 1	4.5	−4.01
DPTD	windmill-shaped pattern	3.5 ± 0.1	3.4 ± 0.1	90 ± 1	-	-

[A] Distance between two molecular aggregations (see figures). [B] Period of the pattern (see figures). [C] Angel between side chain axis and the packing orientation.

(5) Coexistence of adlayer and graphite lattice

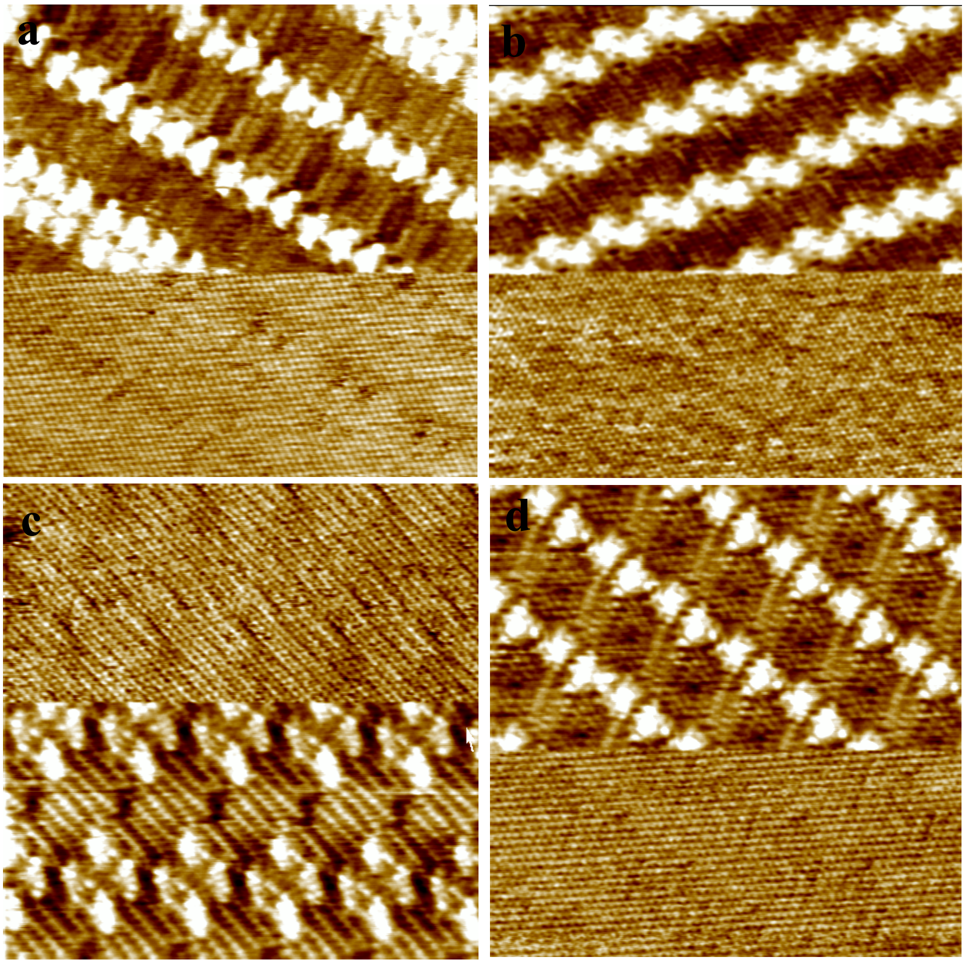

Fig. S16 Composite STM images showing the underlying HOPG lattice and the observed structures of DDTD monolayers. (a) alternate pattern (16 × 16 nm^2). V_{bias} = 570 mV, I_t = 425 pA; (b) dislocated linear pattern (15 × 15 nm^2). V_{bias} = 480 mV, I_t = 360 pA; (c) tetramer pattern (15 × 15 nm^2). V_{bias} = 595 mV, I_t = 420 pA; (d) linear pattern (15 × 15 nm^2). V_{bias} = 523 mV, I_t = 415 pA.

(6) Self-assembly of DDTD-14 in 1-octanoic acid

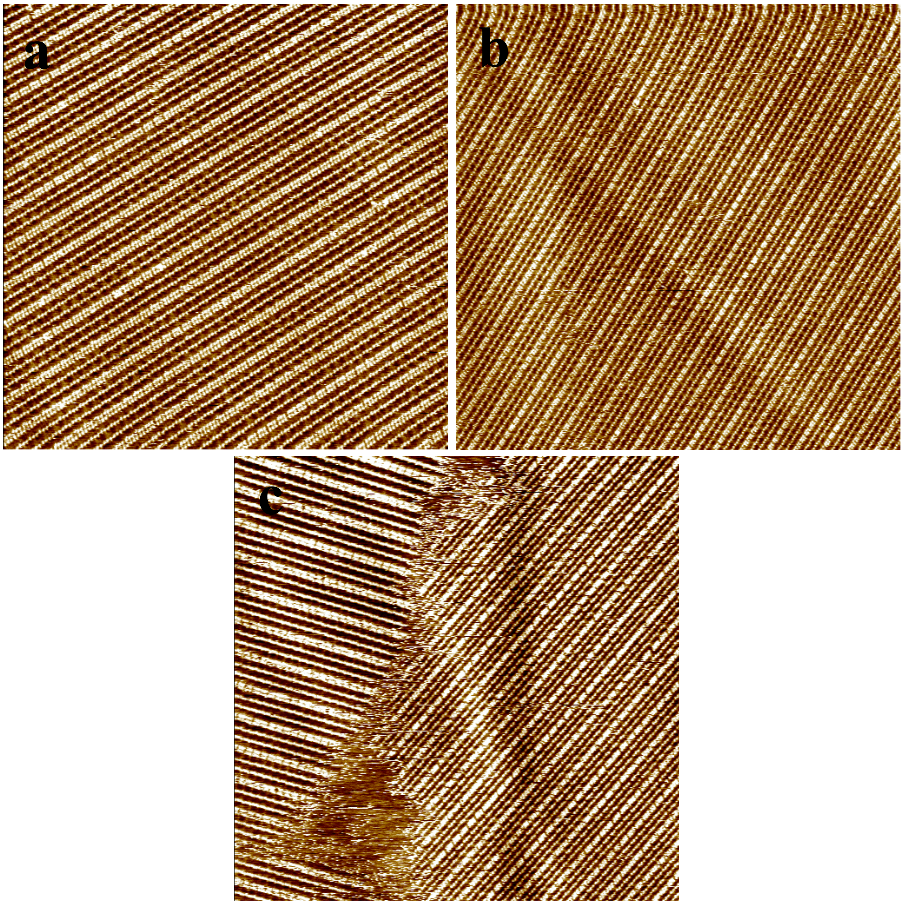

Fig. S17 Large-scale (a) (145 × 145 nm^2) and (b, c) (200 × 200 nm^2) STM images of DDTD-14 self-assembled patterns under different concentrations at the 1-octanoic acid/graphite interface . (a) 7.5 × 10^{-4} mol L^{-1}; (c) 1.25 × 10^{-4} mol L^{-1}; (d) 4.5 × 10^{-5} mol L^{-1}. Ambient temperature is 20 ºC. V_{bias} = 500-600 mV, I_t = 400-450 pA.

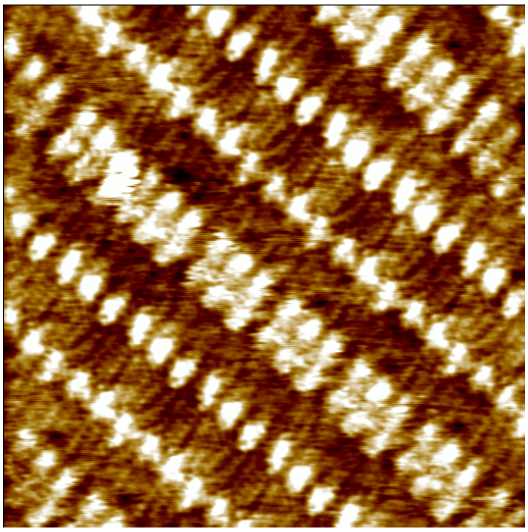

Fig. S18 High-resolution STM image (20× 20 nm^2) of DDTD-14 adlayer at the 1-octanoic acid/graphite interface.

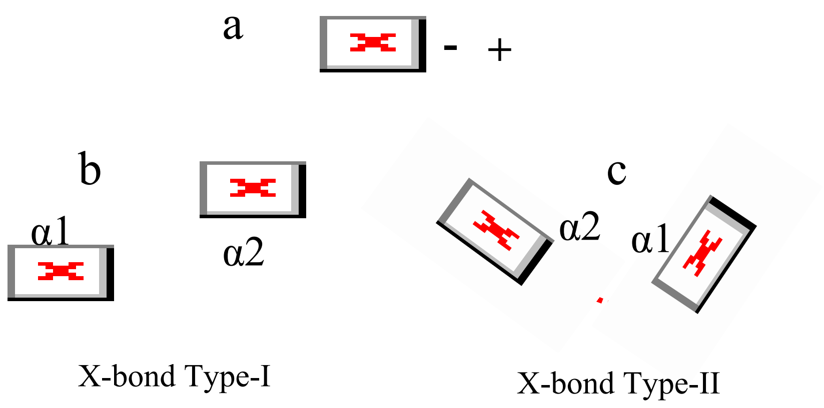

Fig. S19 (a) Charge distribution in the Br-C bond. (b) Type-I halogen bonding. ($\alpha 1 = \alpha 2$). (c) Type-II halogen bonding. ($\alpha 1 \approx 90^{o}$, $\alpha 2 \approx 180^{o}$).

(7) DFT Calculations for the halogen bonding

a

b

E0 = −6611.8774153 a.u

E1 = −13223.7666166 a.u

c

d

E2 = −13223.7666166 a.u

E3 = −13223.761351 a.u

Fig. S20 Atomic structure of (a) single molecule (b) dislocated, (c) tetrameric, and (d) linear configuration obtained from DFT calculations. The calculated energy was indicated in each figure.

The binding energy was calculated as below.

△E1 = E1−2E0= −0.0118166 a.u= −7.4150288 kcal/mol = −0.3215 eV

△E2 = E2−4E0= −0.0351229 a.u= −22.039953 kcal/mol = −0.9557 eV

$\triangle E3 = E3 - 2E0 = -0.006390342$ a.u $= -4.01000031$ kcal/mol $= -0.1062$ eV